

Dielectric and pyroelectric properties of Li_2CO_3 doped $0.2\text{Pb}(\text{Mg}_{1/3}\text{Nb}_{2/3})\text{O}_3-0.5\text{Pb}(\text{Zr}_{0.48}\text{Ti}_{0.52})\text{O}_3-0.3\text{Pb}(\text{Fe}_{1/3}\text{Nb}_{2/3})\text{O}_3$ ceramics

Sun Hee Kang · Chang Won Ahn · Hai Joon Lee ·
Ill Won Kim · Eun Chul Park · Jae Shin Lee

Received: 27 June 2005 / Accepted: 28 December 2005 / Published online: 3 May 2008
© Springer Science + Business Media, LLC 2008

Abstract Relaxor ferroelectric compositions of $0.2\text{Pb}(\text{Mg}_{1/3}\text{Nb}_{2/3})\text{O}_3-0.5\text{Pb}(\text{Zr}_{0.48}\text{Ti}_{0.52})\text{O}_3-0.3\text{Pb}(\text{Fe}_{1/3}\text{Nb}_{2/3})\text{O}_3$ ($0.2\text{PMN}-0.5\text{PZT}-0.3\text{PFN}$) ceramics were doped with different concentrations of Li_2CO_3 and were prepared by a columbite precursor process. Their structural, dielectric and pyroelectric properties were studied. A phase analysis was performed using the X-ray diffraction patterns from $2\theta=44^\circ$ to 46° , over which the tetragonal phase displays two peaks, $(002)_T$ and $(200)_T$, while the rhombohedral phase displays one peak, $(200)_R$. A well saturated $P-E$ hysteresis loop was obtained for the $0.2\text{PMN}-0.5\text{PZT}-0.3\text{PFN}$ ceramic doped with 0.2 wt.% Li_2CO_3 , and the values for the remnant polarization (P_r) and coercive field (E_c) were $30 \mu\text{C}/\text{cm}^2$ and $5.4 \text{ kV}/\text{cm}$, respectively. A maximum value of the pyroelectric coefficient, $518 \mu\text{C}/\text{m}^2\text{K}$, was obtained for the $0.2\text{PMN}-0.5\text{PZT}-0.3\text{PFN}$ ceramic doped with 0.3 wt.% Li_2CO_3 at the maximum temperature (T_{max}) due to the decrease of the binding energy for the polarization charge which in formed at the surface.

Keywords Ferroelectrics · Pyroelectricity ·
 $\text{PMN}-\text{PZT}-\text{PFN}+\text{Li}_2\text{CO}_3$ ceramics

1 Introduction

Lead magnesium niobate, $\text{Pb}(\text{Mg}_{1/3}\text{Nb}_{2/3})\text{O}_3$ (PMN) [1, 2] and lead zirconium titanium, $\text{Pb}(\text{Zr,Ti})\text{O}_3$ (PZT) are the most widely studied prototype relaxor ferroelectric compounds for piezoelectric and pyroelectric devices [3–6]. $\text{Pb}(\text{Mg}_{1/3}\text{Nb}_{2/3})\text{O}_3-\text{Pb}(\text{Zr,Ti})\text{O}_3$ and $\text{Pb}(\text{Fe}_{1/3}\text{Nb}_{2/3})\text{O}_3$ (PFN) are lead based ferroelectrics belonging to the relaxor family. A unique characteristic of relaxors is a broad and frequency dependent diffuse phase transition. Relaxors also exhibit a low thermal expansion behavior up to the Curie temperature (T_C). $\text{Pb}(\text{Fe}_{1/3}\text{Nb}_{2/3})\text{O}_3$, a lead-based complex perovskite, is regarded as a good candidate for multilayer ceramic capacitors owing to its high dielectric constant and low sintering temperature. Due to its intermediate position between the normal ferroelectric ($\text{Pb}(\text{Zr,Ti})\text{O}_3$ materials, BaTiO_3 , SrTiO_3) and the relaxor ferroelectric $\text{Pb}(\text{Mg}_{1/3}\text{Nb}_{2/3})\text{O}_3$) materials, PFN is a promising material from which the relaxor mechanism may be elucidated.

Li_2CO_3 can introduce the presence of a liquid phase and it is helpful to the sintering process [7, 8]. Because the volume of this liquid phase is not large enough for a uniform distribution on the surfaces of all the grains, segregations can result and the concentration gradient of this liquid phase may lead to an abnormal grain growth. The Li^+ cations will tend to occupy the octahedral sites of the perovskite lattice, forming additional anionic vacancies. The anionic vacancies resulting from Li_2CO_3 will then be partially occupied by oxygen which aids the grain growth. In this work, we have fabricated a ternary compound system of the $0.2\text{Pb}(\text{Mg}_{1/3}\text{Nb}_{2/3})\text{O}_3-0.5\text{Pb}(\text{Zr}_{0.48}\text{Ti}_{0.52})\text{O}_3-0.3\text{Pb}(\text{Fe}_{1/3}\text{Nb}_{2/3})\text{O}_3$ ceramics with different Li_2CO_3 doping concentrations using the columbite precursor method and have studied the dielectric, ferroelectric and pyroelectric properties.

S. H. Kang · C. W. Ahn · H. J. Lee · I. W. Kim (✉)
Department of Physics, University of Ulsan,
Ulsan 680-749, South Korea
e-mail: kimiw@mail.ulsan.ac.kr

E. C. Park · J. S. Lee
School of Materials Science and Engineering,
University of Ulsan,
Ulsan 680-749, South Korea

2 Experiment

The 0.2PMN–0.5PZT–0.3PFN ceramics that were modified with Li_2CO_3 were prepared using the columbite precursor method. High purity MgO , Nb_2O_5 , Fe_2O_5 , ZrO_2 and TiO_2 (99.9%) powders were weighed and calcined at 1100 °C for 2 h to form the columbite phases of MgNb_2O_5 and FeNbO_4 . The appropriate amounts of PbO were weighed and mixed with the calcined powders by ball milling for 24 h. After the powders were calcined at 850 °C for 2 h, Li_2CO_3 was doped as a liquid-phase sintering aid. The specimens were sintered from 900 °C to 1100 °C for 2 h in a covered alumina crucible. The details of sample preparation and characterization are given in our earlier communication [9].

X-ray diffraction (XRD) with $\text{Cu-K}\alpha$ radiation was used to characterize the structural phases of the samples. The ferroelectric P – E hysteresis loops were investigated using a Sawyer–Tower circuit. The dielectric constant and loss were measured by an impedance analyzer (HP4192) from room temperature to 400 °C with a heating rate of 2 °C/min. Before measuring the pyroelectric properties, the samples were poled in a silicon oil bath at 150 °C by applying a DC electric field of 4 kV/mm for 30 min. The pyroelectric properties were measured by using the Byer–Round method using a Keithley 237 (source/measure unit electrometer) interfaced with a computer at a constant heating rate of 5 °C/min.

3 Results and discussion

Figure 1 shows the typical XRD patterns of the 0.2PMN–0.5PZT–0.3PFN ceramics doped with different Li_2CO_3 concentrations sintered at 900 °C and an undoped sample sintered at 1100 °C. All samples had the typical perovskite structure, but the sample doped with 0.3 wt.% Li_2CO_3

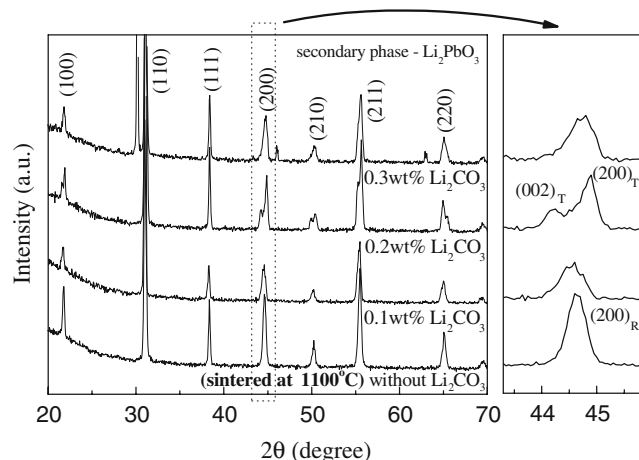
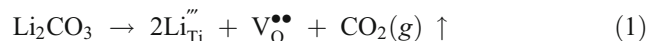
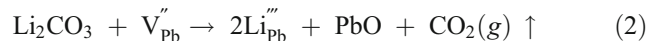


Fig. 1 XRD patterns of the 0.2PMN–0.5PZT–0.3PFN ceramics at various Li_2CO_3 doping contents

showed a secondary phase of Li_2PbO_3 . The phase analysis was performed from the XRD patterns over a range of $2\theta = 44^\circ$ to 46° , where the tetragonal phase displays two peaks, $(002)_T$ and $(200)_T$, and the rhombohedral phase displays one peak, $(200)_R$. The sample that was not doped with Li_2CO_3 exhibited a rhombohedral phase, but the samples doped with Li_2CO_3 showed the tetragonal phase. There was a broad region where the two phases, rhombohedral and tetragonal, coexisted which indicated typical morphotropic phase behavior (MPB). For the compositions studied here, the composition closest to the morphotropic phase boundary was found to be 0.2PMN–0.5PZT–0.3PFN ceramics doped with 0.1 and 0.2 wt.% Li_2CO_3 . The probability polyhedron model developed by Cao and Cross [10] correlated a larger grain size with a narrower region of composition for the coexistence of the two phases at the MPB. For the samples doped with 0.1 wt.% Li^{1+} and greater, the main PMN–PZT–PFN phase changed from a rhombohedral to a tetragonal structure. For the rhombohedral region, the substitution of Li^{1+} caused a reduction of lattice constant (c/a), but in the tetragonal region, the addition of Li^{1+} gave rise into a linear increase of the tetragonality ratio by c/a . So, we supposed two cases about the substitutions of Li^{1+} for the A and B-site. First, the substitution of Li^{1+} for the Ti^{4+} (B-site) enhanced the c/a ratio. The Li^{1+} cations tend to occupy the octahedral sites of the perovskite lattice, forming additional anionic vacancies, according to the following Eq. 1



The anionic vacancies coming from Li_2CO_3 will then be partially occupied by oxygen. This is helpful for the grain growth. This causes a distortion in the lattice. So, the substitution of Li^{1+} cations in Ti^{4+} site let the c -axis be lengthened. Second, the Li_2CO_3 ion replaced at the A-site and B-site simultaneous. Li^{1+} cations act as acceptor additives, with low valance and small radius. Li^{1+} cations will substituted into Pb site and the escaped Pb^{2+} cations from that sites will combine with oxygen to form a PbO at the same time, according to the following Eq. 2.



If Li^{1+} cations substitute into Ti^{4+} site, then the Ti^{4+} cations which were come out from the lattice will combine with oxygen to form a TiO_2 , according to the following Eq. 3.



The reacted PbO and TiO_2 will be synthesized into tetragonal PbTiO_3 with the help of thermal energy which is being supplied during the sintering process. A rhombohedral phase of PMN–PZT–PFN hence will turn into tetragonal ones. This is well agreed with the result of Lei et al. [11].

Figure 2 shows the temperature dependence of the dielectric constant and loss at 100 kHz for the 0.2PMN–0.5PZT–0.3PFN+Li₂CO₃ ceramics sintered at 900 °C and a pure sample sintered at 1100 °C. The maximum dielectric constant at the Curie temperature (*T_C*) increased with increasing 0.2 wt.% Li₂CO₃ concentration and decreased at 0.3 wt.% Li₂CO₃. The *T_C* values were 220 °C and 208 °C for the 0.2PMN–0.5PZT–0.3PFN and 0.2PMN–0.5PZT–0.3PFN+x wt.% Li₂CO₃ ceramics, respectively. The 0.2PMN–0.5PZT–0.3PFN sample doped with 0.2 wt.% Li₂O₃ showed a fairly high dielectric constant ($\epsilon=28000$) at room temperature, and low dielectric dissipation factor ($\tan \delta=0.02$) at the Curie temperature. Any further increase of the Li₂CO₃ concentration appeared to be detrimental, as evidenced by the considerably lowered dielectric constant. For the ceramics doped with the Li₂CO₃ concentrations higher than 0.3 wt.%, the maximum values of the dielectric constant was reduced, even with the occurrence of the pyrochlore phase, and this was attributed to the detrimental effects resulting from the addition of Li₂CO₃. Chen and coworkers [12, 13] reported that the decrease in the dielectric constant is not only due to pyrochlore phase but also other factors such as lattice impurities and inter-granular phases.

Figure 3 shows the ferroelectric polarization–electric field (*P–E*) loops of the 0.2PMN–0.5PZT–0.3PFN ceramics doped with different Li₂CO₃ concentrations at room temperature. The inserted figure shows the variation of the remnant polarization (*P_r*) and coercive field (*E_c*) as a function of the Li₂CO₃ ratio. The *P_r* of the 0.2PMN–0.5PZT–0.3PFN ceramics increased with increasing Li₂CO₃ up to 0.2 wt.% and then decreased at 0.3 wt.% Li₂CO₃. The shape of the hysteresis loops changed from slip to rectangular with increasing Li₂CO₃. It is well known that the polarization vector at the rhombohedral phase is (111)_R and has eight directions for the dipole moment

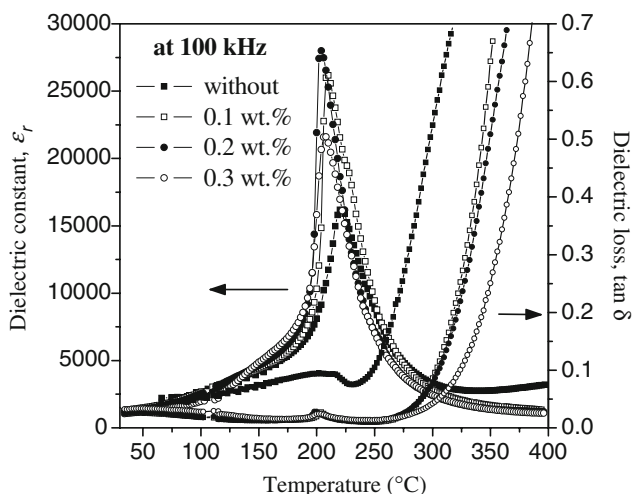


Fig. 2 The dielectric constant and loss of the 0.2PMN–0.5PZT–0.3PFN ceramics at various Li₂CO₃ doping contents

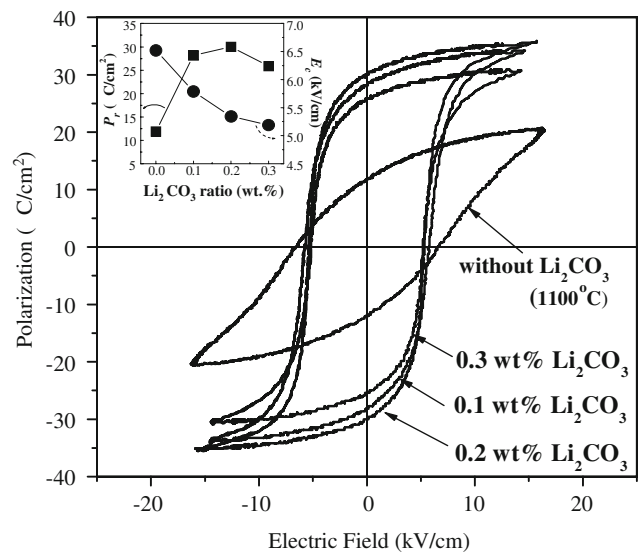


Fig. 3 The variations in the *P–E* hysteresis loops of the 0.2PMN–0.5PZT–0.3PFN ceramics as a function of the electric field at various Li₂CO₃ doping contents

reorientation. Similarly the polarization vector (001)_T for the tetragonal phase has six directions for the dipole moment reorientation. Because the rhombohedral and tetragonal phases coexisted in the 0.2 wt.% Li₂CO₃ doped sample, there were 14 directions for the dipole moment reorientation. Thus the remnant polarization of the sample doped with 0.2 wt.% Li₂CO₃ was higher than those of the rhombohedral or tetragonal phases alone. Well saturated *P–E* hysteresis loop with rectangular shapes were obtained and the maximum value of the *P_r* was 30 $\mu\text{C}/\text{cm}^2$ in the 0.2PMN–0.5PZT–0.3PFN+0.2 wt.% Li₂CO₃ ceramic.

Figure 4 shows the temperature dependence of the pyroelectric coefficient for the base composition that was modified by doping with 0 to 0.3 wt.% Li₂CO₃. The maximum pyroelectric coefficients increased with increasing

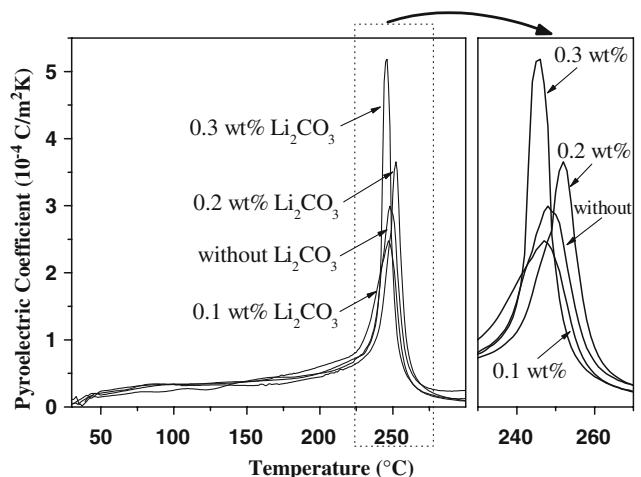


Fig. 4 The pyroelectric coefficient of the 0.2PMN–0.5PZT–0.3PFN ceramics at various Li₂CO₃ doping contents

Li_2CO_3 contents up to 0.3 wt.%. The pyroelectric properties of the 0.2PMN–0.5PZT–0.3PFN+ Li_2CO_3 samples improved with increasing the concentrations of Li_2CO_3 which differed from the results obtained from dielectric and ferroelectric measurements. In the case of the sample containing 0.3 wt.% Li_2CO_3 , the crystalline structure did not change directly from fluorite to perovskite in the firing process but formed a pyrochlore phase due to the excess of Li_2CO_3 and an oxygen vacancy instead. The dipole moment of the metastable pyrochlore phase can be easily reoriented because of the large pyroelectric current occurred with only a small temperature variation due to a decrease of the binding energy of the polarization charge which is formed at the sample surface. One salient feature of the data is that the temperature with a maximum dielectric constant (T_C) does not coincide with the temperature at which a maximum pyroelectric coefficient maximum temperature (T_{max}) is achieved. This difference is a feature distinctly different from that of normal first-order ferroelectrics. Unlike first-order ferroelectrics, the relaxors depolarize at a temperature (T_{max}) which is lower than the dielectric peak temperature (T_C). The difference between T_C and T_{max} increases as the Li_2CO_3 content increases. This means that the diffuseness of the phase transition increases with increasing Li_2CO_3 . Maximum values of the pyroelectric coefficient were obtained from the 0.2PMN–0.5PZT–0.3PFN sample doped with 0.3 wt.% Li_2O_3 with $518 \mu\text{C}/\text{m}^2\text{K}$ at the T_{max} due to a decrease of the binding energy for the polarization charge which in formed at the surface.

4 Conclusions

A phase analysis of 0.2PMN–0.5PZT–0.3PFN ceramics was performed using the XRD patterns. The sample without Li_2CO_3 exhibited the rhombohedral phase, but the

samples doped with Li_2CO_3 exhibited the tetragonal phase. At room temperature, the 0.2PMN–0.5PZT–0.3PFN sample doped with 0.2 wt.% Li_2O_3 had a fairly high dielectric constant ($\epsilon=28000$) and a low dielectric dissipation factor ($\tan \delta=0.02$) at the Curie temperature. A well saturated P – E hysteresis loop with a rectangular shape was obtained with a maximal value of P_r ($30 \mu\text{C}/\text{cm}^2$) in the 0.2PMN–0.5PZT–0.3PFN+0.2 wt.% Li_2CO_3 MPB sample. Maximum values for the pyroelectric coefficient were obtained in the 0.3 wt.% Li_2O_3 doped 0.2PMN–0.5PZT–0.3PFN sample with $518 \mu\text{C}/\text{m}^2\text{K}$ at the T_{max} . This was due to a decrease the binding energy of the polarization charge which formed at the surface.

Acknowledgments This research was supported by a grant from Center for Advanced Materials Processing of 21st Century Frontier R and D Program funded by the Ministry of Science and Technology, Republic of Korea.

References

1. S. Ananta, N.W. Thomas, J. Eur. Ceram. Soc **19**, 2917 (1999)
2. S.B. Lee, S.H. Yoon, H. Kim, J. Eur. Ceram. Soc **24**, 2465 (2004)
3. R.W. Whatmore, Rep. Prog. Phys **49**, 1335 (1986)
4. R.W. Whatmore, Ferroelectrics **118**, 241 (1991)
5. S.B. Stringfellow, S. Gupta, C. Shaw, J.R. Alcock, R.W. Whatmore, J. Eur. Ceram. Soc **22**, 573 (2002)
6. J.M. Jung, S.W. Choi, Jpn. J. Appl. Phys **37**, 5261 (1998)
7. D.L. Corker, R.W. Whatmore, E. Ringgaard, W.W. Wolny, J. Eur. Ceram. Soc **20**, 2039 (2000)
8. Q.L. Jianquan Qi, Y. Wang, Z. Gui, L. Li, J. Eur. Ceram. Soc **21**, 2217 (2001)
9. J.S. Lee, E.C. Park, S.H. Lee, D.S. Lee, Y.J. Lee, J.S. Kim, I.W. Kim, B.M. Jin, Mater. Chem. Phys **90**, 381 (2005)
10. W. Cao, L.E. Cross, Phys. Rev. B **47**(9), 4825 (1993)
11. C. Lei, K. Chen, X. Zhang, Mat. Sci. Eng **B111**, 107 (2004)
12. J. Chen, M.P. Harmer, J. Am. Ceram. Soc **73**, 68 (1990)
13. J. Chen, A. Gorton, H.M. Chen, M.P. Harmer, J. Am. Ceram. Soc **69**, C303 (1986)